Electronic Supplementary Material (ESI) for ChemComm.

Supporting Information

Facile one-step dialysis strategy for fabrication of hollow complex nanoparticles

Lili Cui,[+a] *Chenchen Wang,*[+a] *Hongwei Zhang,*[a] *Yunsheng Ma,*[b] *Guang Deng,*[a] *Zhiguo Zhou,*[a] *Jiaomin Lin,**[a] *Hong Yang,**[a] *and Shiping Yang**[a]

[a]The Education Ministry Key Lab of Resource Chemistry and Shanghai Key Laboratory of Rare Earth Functional Materials, Shanghai Normal University, Shanghai 200234, China

[b]School of Chemistry and Materials Engineering, Jiangsu Key Laboratory of Advanced Functional Materials, Changshu Institute of Technology, Changshu, Jiangsu 215500, China

Experimental Section

1.1 Materials

2-phenylquionline (pq), iridium trichloride hydrate and rare-earth salt were purchased from J&K Scientific. Polyvinylpyrrolidone (PVP, Mw = 45000−55000) were obtained from Shanghai Sinopharm Chemical Reagent Co., Ltd. The other reagents were obtained from TiTan. Ultrapure deionized water (18.2 MΩ resistivity) from a Millipore system was used. $[Ir(pq)_2(bpy)]Cl$ (**1**) and $[(pq)_2Ir(H_2dcppy)]Cl$ (**2**) were synthesized according to the previous literature[1]. Crystals of **2** were obtained by slowly diffusion of diethyl ether solution to the dichloromethane solution contained complex **2**.

1.2 Characterization

Scanning electron microscope (SEM) images for the nanoparticles were determined on a Hitachi Hitachi S-4800 SEM. The ultrasonic imaging was performed on a MyLab Twice ultrasonic diagnostic instrument using a typical B mode (Esaote SpA, Genova, Italy). The measurement of the hydrodynamic diameter and surface potential of the nanoparticles were carried out on Malvern Zetasizer Nano ZS. Transmission electron microscopy (TEM) images were measured on a JEOL JEM-2100 TEM. Powder X-ray diffraction (PXRD) data were measured using an ADVANCE X-ray powder diffractometer (Bruker D8).

The diffraction data for complex **2** and **3** were collected using a Bruker single-crystal diffractometer with Mo-Kα radiation (λ = 0.71073 Å). The absorption corrections for the data were carried out using the SADABS program. The structures were solved by the direct method and refined using the full-matrix least-squares technique on F^2 by the SHELXTL package. All non-hydrogen atoms were refined anisotropically and hydrogen atoms were placed geometrically. The crystallographic data for this paper were delivered to Cambridge Crystallographic Data Centre (CCDC) with No. of 1882239 and 1919897 for complex **2** and **3**, respectively. These data can be obtained from the CCDC via www.ccdc.cam.ac.uk/data_request/cif.

1.3 Synthesis of complex $[Ir_4Ho_2(pq)_8(dcbpy)_4(OAc)_2]$ (3)

$[(pq)_2Ir(H_2dcppy)]Cl$ (**2**) (0.009 mmol, 7.3 mg) and $Ho(OAc)_3$ (0.025 mmol, 9 mg) in DMF/MeOH (1 mL/1 mL) were added into a 5 mL glass vial and placed in the Teflon autoclave at 90 °C for 2 d. Red crystals of $[Ir_4Ho_2(pq)_8(dcbpy)_4(OAc)_2]$ (**3**) were obtained after cooled to room temperature.

1.4 Synthesis of hollow complex nanoparticles

In a flask contained 5 mL of DMSO, 3.5 mg of $[Ir(pq)_2(bpy)]Cl$ (**1**) was dissolved at 110 ^oC, following by cooled down to room temperature and then transfered into a dialysis bag with MWCO of 8000-14000. This dialysis bag was then dialyzed against deionized water at 25 ^oC for 12 h. The nanoparticles were collected through centrifugation.

The procedure for the synthesis of $[(pq)_2Ir(H_2dcppy)]Cl$ (**2**) and $[Ir_4Ho_2(pq)_8(H_2dcbpy)_4(OAc)_2]$ (**3**) was similar to that of **1**, excepting the complexes of **2** and **3** were adopted, respectively.

1.5 Synthesis of rare-earth-Ir hybrid nanoparticles (HNPs)

In a flask, 3.5 mg of complex **2** (0.004 mmol) and 2.1 mg of $Dy(OAc)_3 \cdot 4H_2O$ (0.005 mmol) were reacted in DMSO (5 mL) at 110 ^oC for 7 h, following by cooled down to room temperature and then transfered into a dialysis bag with MWCO of 8000-14000. This dialysis bag was then dialyzed against deionized water at 25 ^oC for 12 h. The nanoparticles were collected through centrifugation. The PVP modified rare-earth-Ir hybrid nanoparticles were synthesized with the similar procedure, excepting 50 mg of PVP (Mw = 45000-55000) were added into the mixture before reaction.
The other rare-earth ions doped nanoparticles were also synthesized using the similar method except different rare earth salts were adopted.

1.6 In vitro MR imaging

In vitro T_2-weighted MR images and the relaxivity transverse relaxation times (T_2) in solution of Ir-Dy HNPs were measured on a 7.0 T MR scanner. The parameters were TR, 1500 ms; TE, 15.6 ms, field of view, 60.0×30.0 mm; slice thickness, 1 mm; matrices, 256×256; bandwidth, 300.3 Hz/Px.

1.7 *In vitro* US imaging

After degassed, the aqueous solution of different concentrations of Ir-Dy HNPs filled in a tank was imaged at room temperature on an ultrasonic diagnostic instrument (ESAMyLab9, Esaote SpA, Genova, Italy). The conventional B mode and CEUS of harmonic with a 522 transducer (centre frequency, 7.5 MHz; mechanical index, 0.10) were used for the imaging. Image J was used for the quantitative analysis of harmonic ultrasonic signal.

1.8 *In vivo* cytotoxicity assay

To evaluate *in vivo* cytotoxicity assay, the Healthy ICR mice that obtained from the Shanghai SLAC Laboratory Animal Co., Ltd were intravenously injected with 200 μL of Ir-Dy HNPs (12 mg/kg body weight). Simultaneously, the mice for the control group were intravenously injected with the same dose of saline. After 24 h and one month injection, respectively, the mice were sacrificed for collecting the blood (1 mL) and the main organs (spleen, lung, heart, kidney and liver). All of the operations of the animal procedures were carried out strictly according to the Regional Ethics Committee for Animal Experiments.

1.9 *In Vivo* MRI imaging

For the MRI imaging, healthy ICR mice that obtained from the Shanghai SLAC Laboratory Animal Co., Ltd were intravenously injected with 200 μL of Ir-Dy HNPs (12 mg/kg body weight). After 1 h injection, T_2-weight imaging of the mice was carried out using a 7.0 T MRI scanner (Siemens Magnetom Trio). The imaging parameters were following: TR/TE, 2245.5/33.0 ms; matrix size, 256 × 256; bandwidth, 300.3 Hz/Px; FOV, 40.0 × 35.0 mm; slice thickness, 1 mm. Relative signal intensity (%) = (signal intensity in liver/signal intensity in muscle)*100%.

1.10 *In vivo* US imaging

After intravenously injected with Ir-Dy HNPs (16 mg/kg body weight) for one hour, the

mice were anesthetized by 10% trichloroacetaldehyde hydrate (200 μL), and then collected US imaging photographs and imaging signals on a small animal US imaging instrument (Prospect, S-Sharp). The imaging parameters were following: Fps, 20 Hz; Freq, 40 MHz; Dynamic range, 50 dB; Power, 90.0 %; Depth, 5.1 mm; Gain, 0 dB. To maintain the body temperature, the mice were kept on a heated stage during imaging.

Table S1 Crystallographic data and structural refinements for complex **2** and **3**.

Complex	$[Ir(pq)_2(H_2dcbpy)]\cdot Cl\cdot(CH_2Cl_2)_2$ (**2**)	$[Ir_4Ho_2(pq)_8(H_2dcbpy)_4(OAc)_2]$ (**3**)
Formula	$Ir_2C_{86}H_{59}Cl_5N_8O_8$	$Ir_4Ho_2C_{178}H_{124}N_8O_{22}$
Formula weight	1894.1	3965.7
Temperature (K)	293(2)	173 (2)
Crystal system	Monoclinic	Monoclinic
Space group	*C*2/*c*	*P*21/*c*
a/Å	31.338(3)	14.342(1)
b/Å	12.394(1)	33.629(2)
c/Å	21.563(2)	15.908(1)
α/°	90	90
β/°	119.014(4)	98.560(2)
γ/°	90	90
V/Å^3	7324.2(12)	7587.2(8)
Z	4	2
D_c /g cm^{-3}	1.718	1.736
reflns coll.	21536	39333
unique reflns	7201	14066
R_{int}	0.0621	0.0742
R_1 [$I > 2\sigma(I)$][a]	0.0433	0.0549
wR_2 [$I > 2\sigma(I)$][b]	0.0934	0.1328
R_1 (all data)	0.0659	0.0788
wR_2 (all data)	0.1031	0.1460
GOF	1.003	1.011

[a] $R_1 = \Sigma||F_o| - |F_c||/\Sigma|F_o|$, [b] $wR_2 = [\Sigma w(F_o^2 - F_c^2)^2/\Sigma w(F_o^2)^2]^{1/2}$.

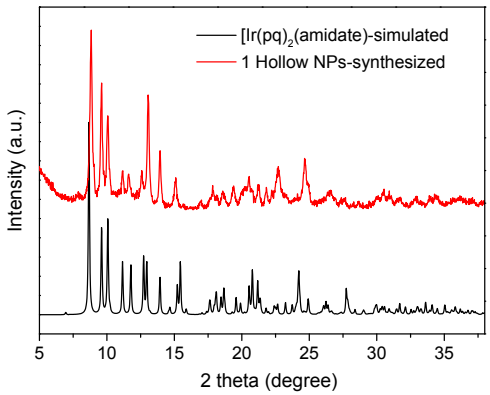

Fig. S1 XRD patterns of the as-synthesized **1** hollow NPs. [Ir(pq)$_2$(amidate)] (amidate = N-(p-tolyl)benzamide) was a Ir-complex with simulated structure of **1** reported by Wang *et al*. [2].

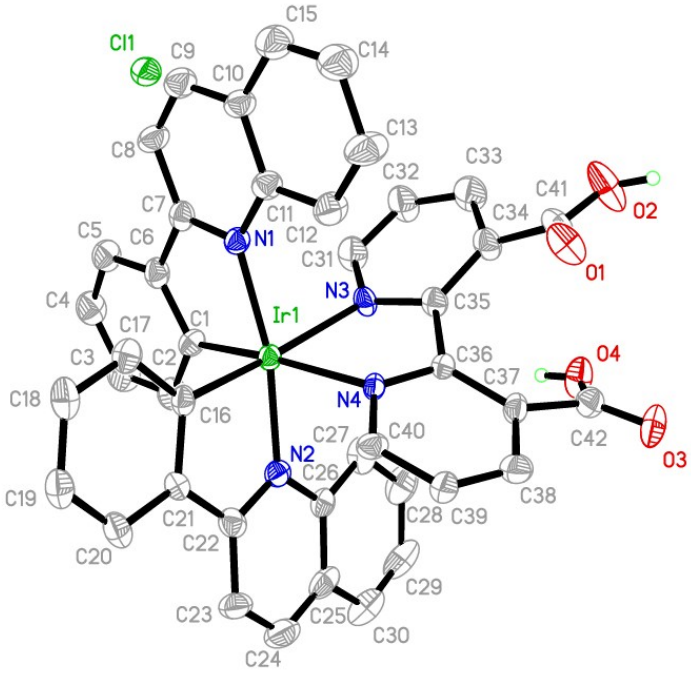

Fig. S2 The drawing of [Ir(pq)$_2$(H$_2$dcbpy)]Cl (**2**). Thermal ellipsoids are drawn at 50% probability level. The solvent molecules of CH_2Cl_2 and hydrogen atoms are omitted.

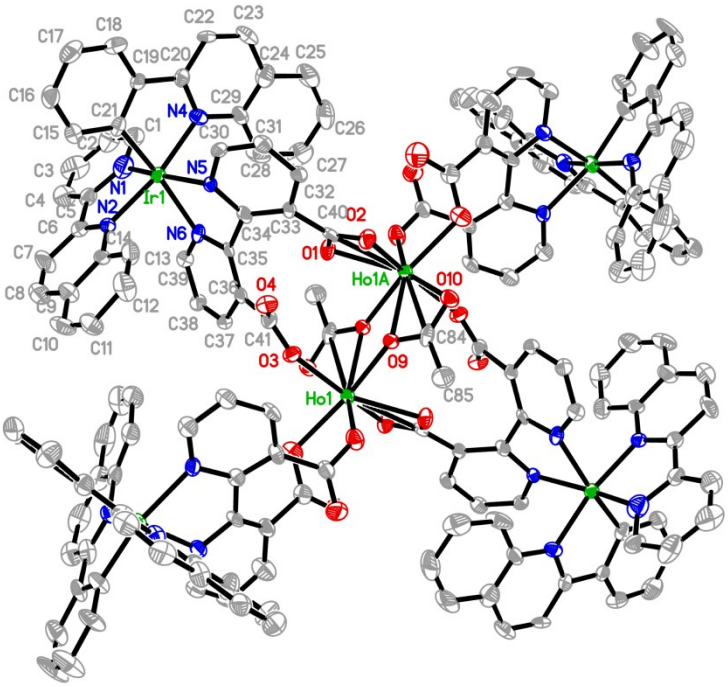

Fig. S3 The drawing of $[Ir_4Ho_2(pq)_8(H_2dcbpy)_4(OAc)_2]$ (**3**). Thermal ellipsoids are drawn at 50% probability level. The solvent molecules of DMF and hydrogen atoms are omitted.

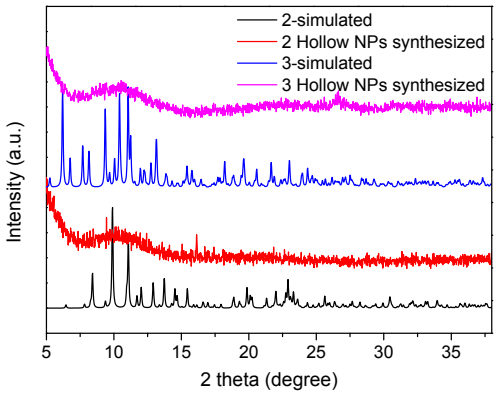

Fig. S4 XRD patterns of the synthesized **2** and **3** hollow NPs.

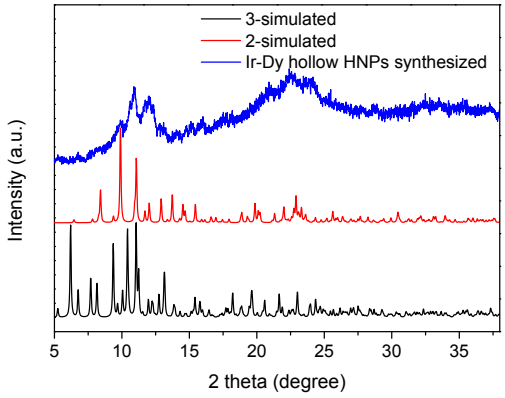

Fig. S5 XRD patterns of Ir-Dy hollow HNPs

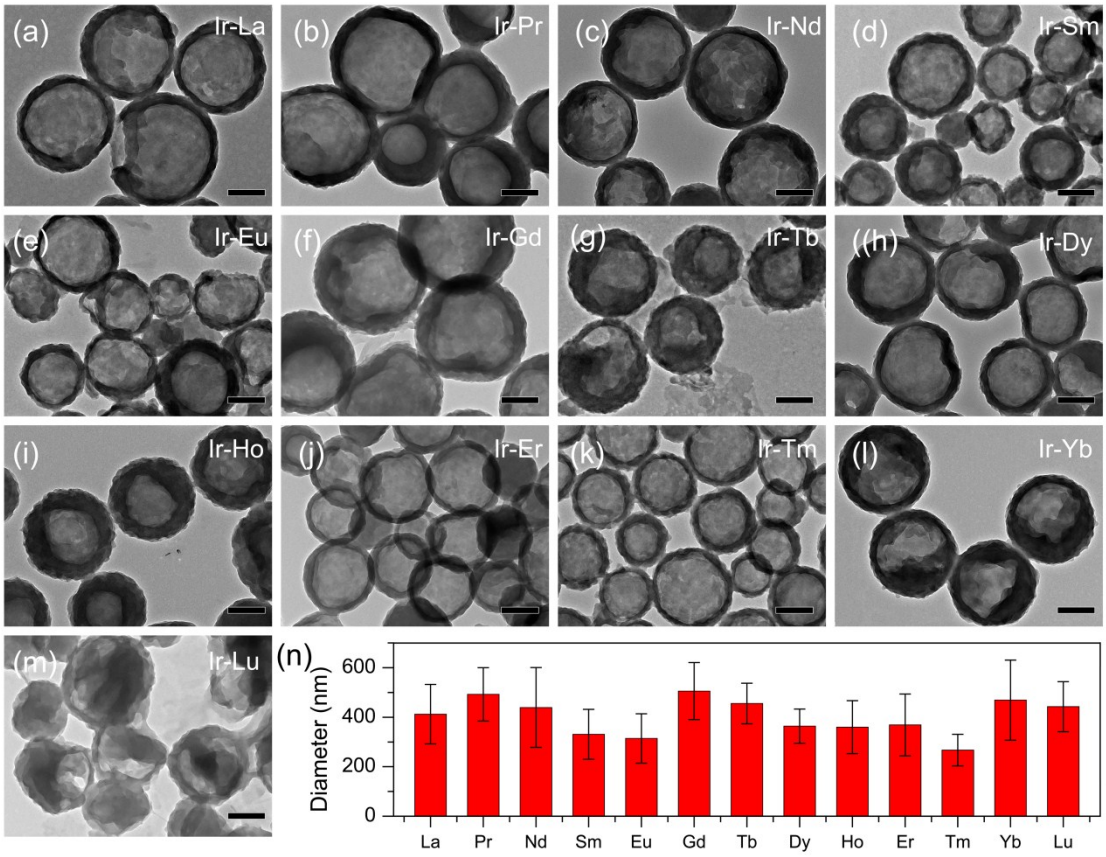

Fig. S6 TEM images of (a) Ir-La HNPs, (b) Ir-Pr HNPs, (c) Ir-Nd HNPs, (d) Ir-Sm HNPs, (e) Ir-Eu HNPs, (f) Ir-Gd HNPs, (g) Ir-Tb HNPs, (h) Ir-Dy HNPs, (i) Ir-Ho HNPs, (j) Ir-Er HNPs, (k) Ir-Tm HNPs, (l) Ir-Yb HNPs, (m) Ir-Lu HNPs synthesized with addtion of PVP. (n) The diameters of the HNPs. The scale bar presents 200 nm.

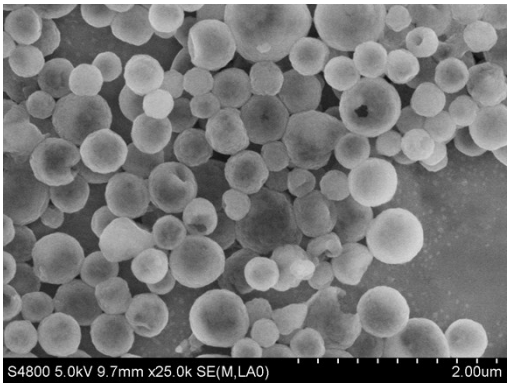

Fig. S7 The SEM image of Ir-La HNPs synthesized with addtion of PVP.

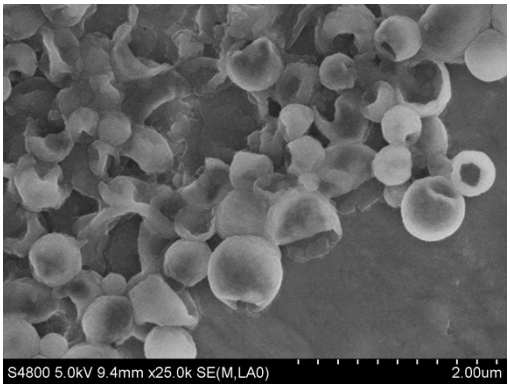

Fig. S8 The SEM image of Ir-Pr HNPs synthesized with addtion of PVP.

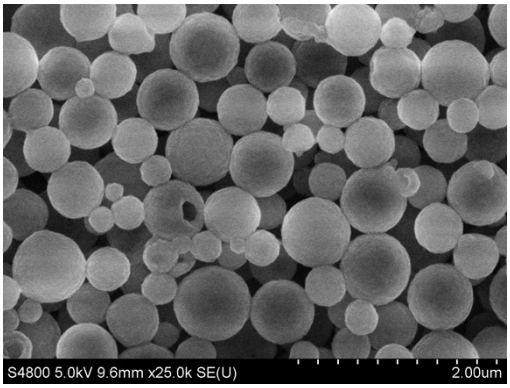

Fig. S9 The SEM image of Ir-Nd HNPs synthesized with addtion of PVP.

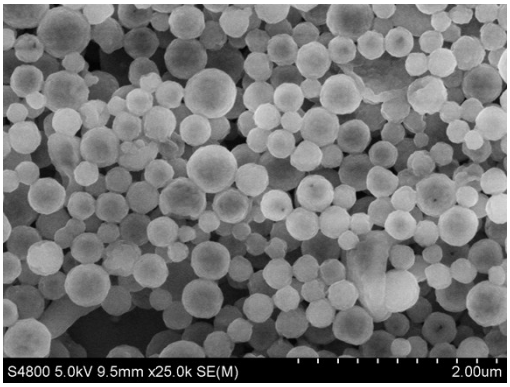

Fig. S10 The SEM image of Ir-Sm HNPs synthesized with addtion of PVP.

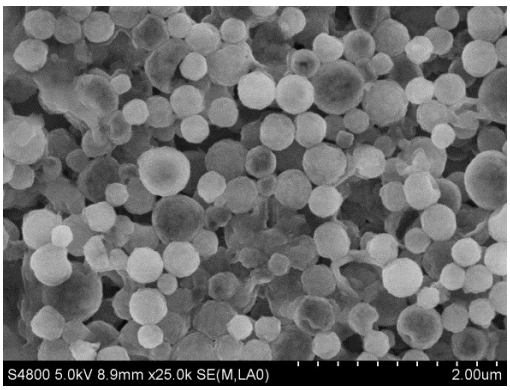

Fig. S11 The SEM image of Ir-Eu HNPs synthesized with addtion of PVP.

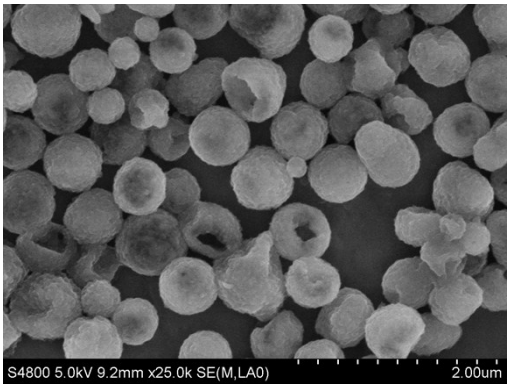

Fig. S12 The SEM image of Ir-Gd HNPs synthesized with addtion of PVP.

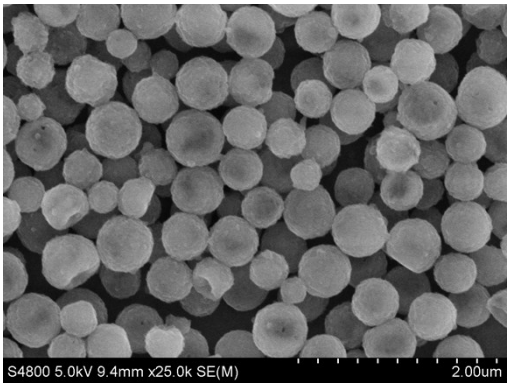

Fig. S13 The SEM image of Ir-Tb HNPs synthesized with addtion of PVP.

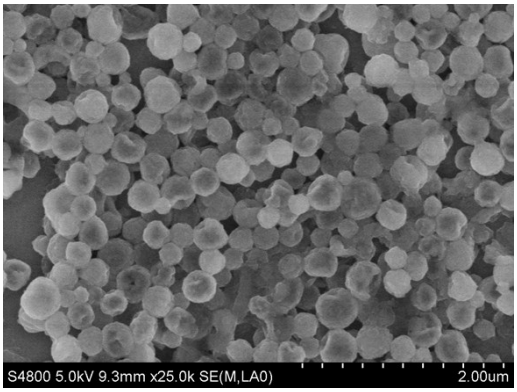

Fig. S14 The SEM image of Ir-Dy HNPs synthesized with addtion of PVP.

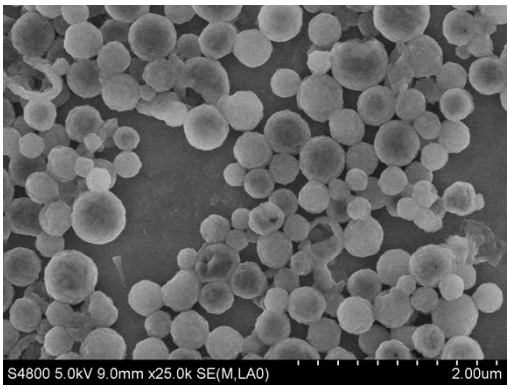

Fig. S15 The SEM image of Ir-Ho HNPs synthesized with addtion of PVP.

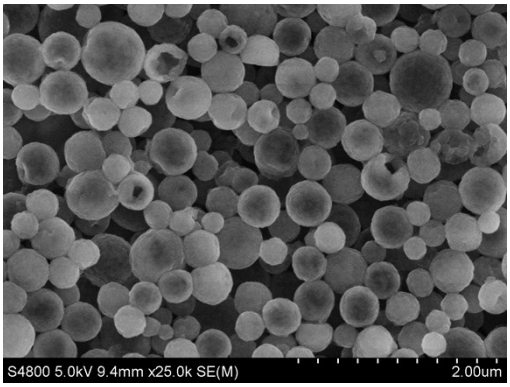

Fig. S16 The SEM image of Ir-Er HNPs synthesized with addtion of PVP.

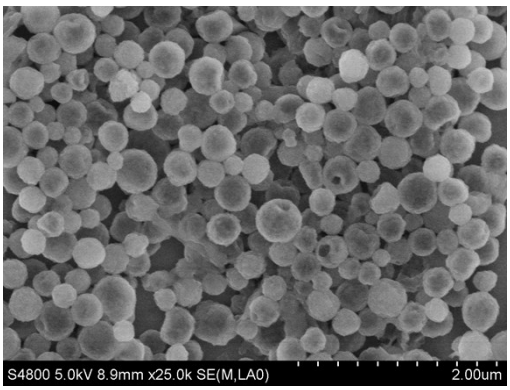

Fig. S17 The SEM image of Ir-Tm HNPs synthesized with addtion of PVP.

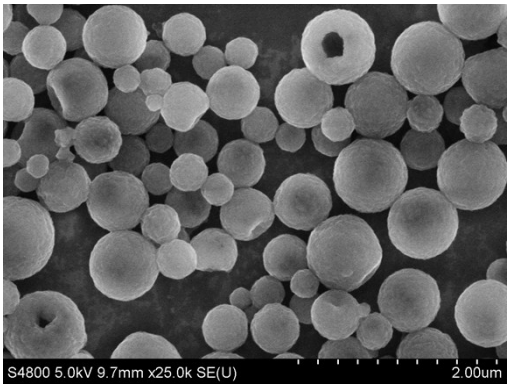

Fig. S18 The SEM image of Ir-Yb HNPs synthesized with addtion of PVP.

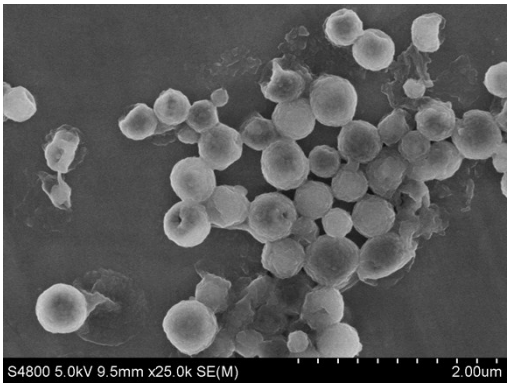

Fig. S19 The SEM image of Ir-Lu HNPs synthesized with addtion of PVP.

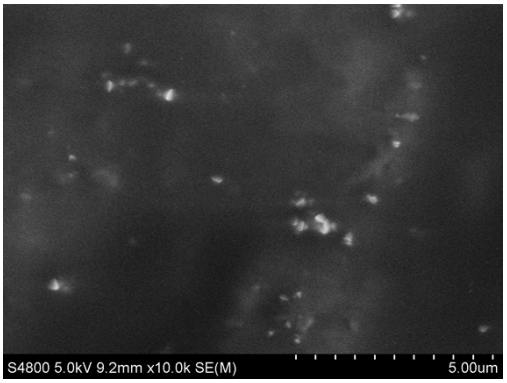

Fig. S20 The SEM image of the mixture of Dy(III) and [$(pq)_2Ir(H_2dcbpy)Cl$] before the dialysis process.

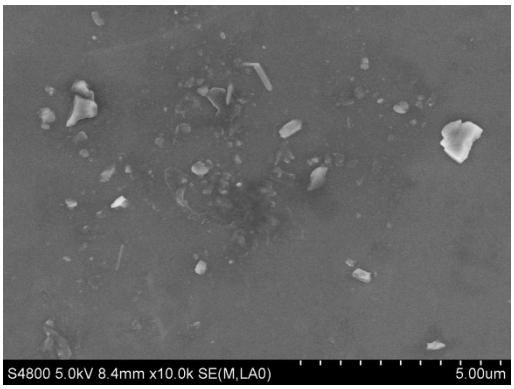

Fig. S21 The SEM image of the mixture of Dy(III) and [$(pq)_2Ir(H_2dcbpy)Cl$] and water.

System

Temperature (°C):	25.1	**Duration Used (s):**	60
Count Rate (kcps):	228.7	**Measurement Position (mm):**	4.65
Cell Description:	Glass cuvette with round ape...	**Attenuator:**	9

Results

			Size (d.n...	% Intensity	Width (d.n...
Z-Average (d.nm):	393.8	**Peak 1:**	354.6	100.0	74.72
PdI:	0.234	**Peak 2:**	0.000	0.0	0.000
Intercept:	0.938	**Peak 3:**	0.000	0.0	0.000
Result quality	Good				

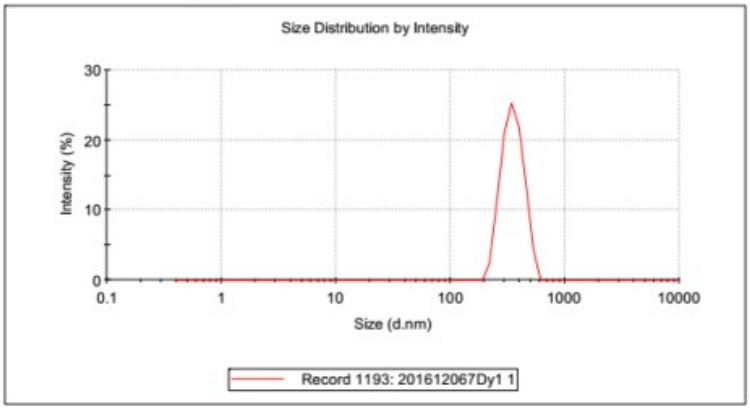

Fig. S22 The hydrodynamic diameter of Ir-Dy HNPs

System

Temperature (°C):	25.1	**Zeta Runs:**	12
Count Rate (kcps):	94.2	**Measurement Position (mm):**	2.00
Cell Description:	Clear disposable zeta cell	**Attenuator:**	7

Results

			Mean (mV)	Area (%)	Width (mV)
Zeta Potential (mV):	-16.6	**Peak 1:**	-16.6	100.0	4.59
Zeta Deviation (mV):	4.59	**Peak 2:**	0.00	0.0	0.00
Conductivity (mS/cm):	0.0178	**Peak 3:**	0.00	0.0	0.00
Result quality	Good				

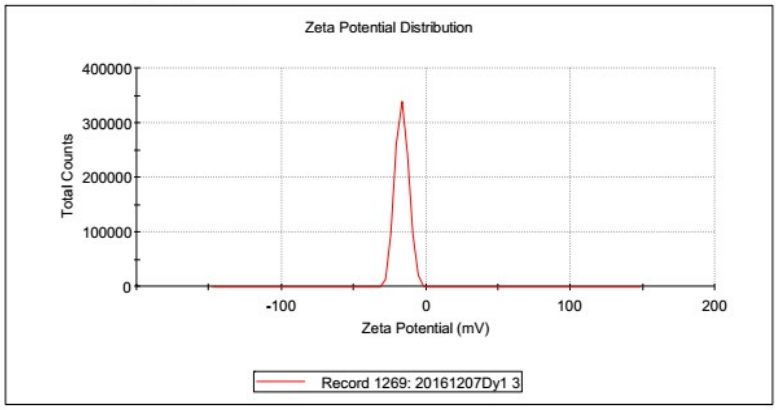

Fig. S23 The Zeta potential of Ir-Dy HNPs

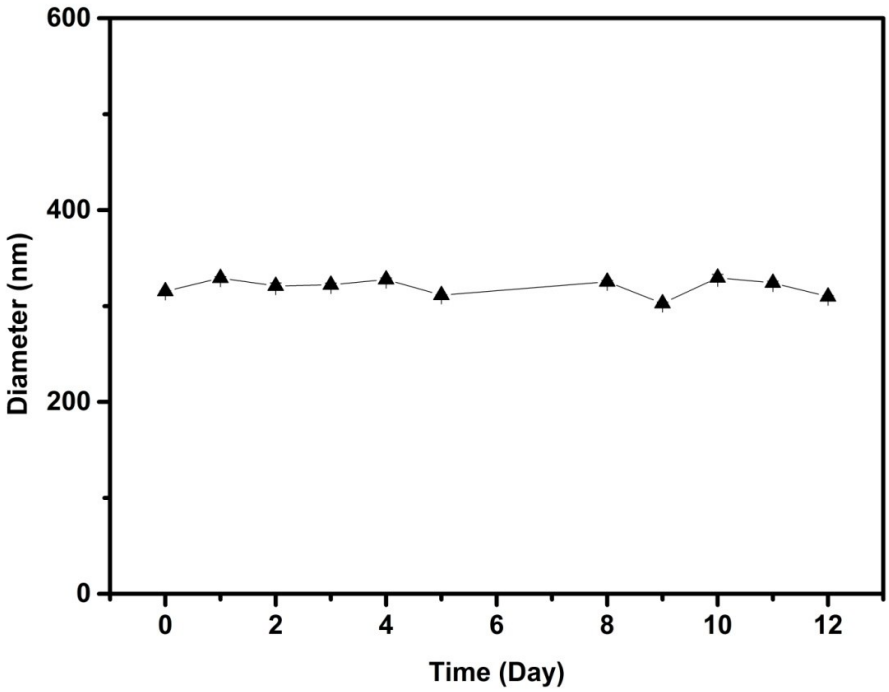

Fig. S24 Time-dependent diameter changes of Ir-Dy HNPs in 1640 plus 10% fetal bovine serum (FBS).

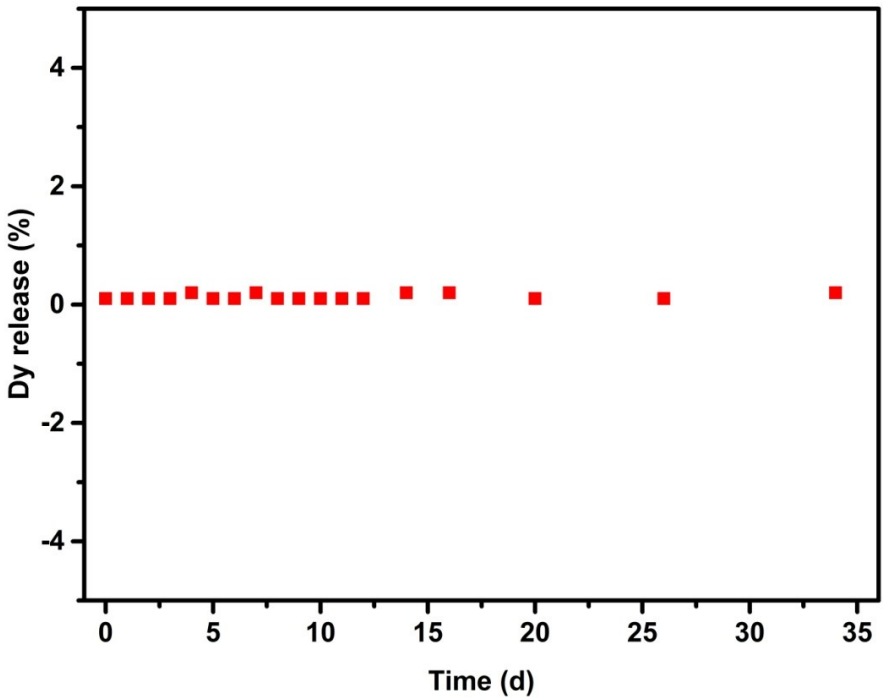

Fig. S25 Time-dependent change of concentrations of Dy(III) ions for Ir-Dy HNPs in 1640 plus 10% fetal bovine serum (FBS).

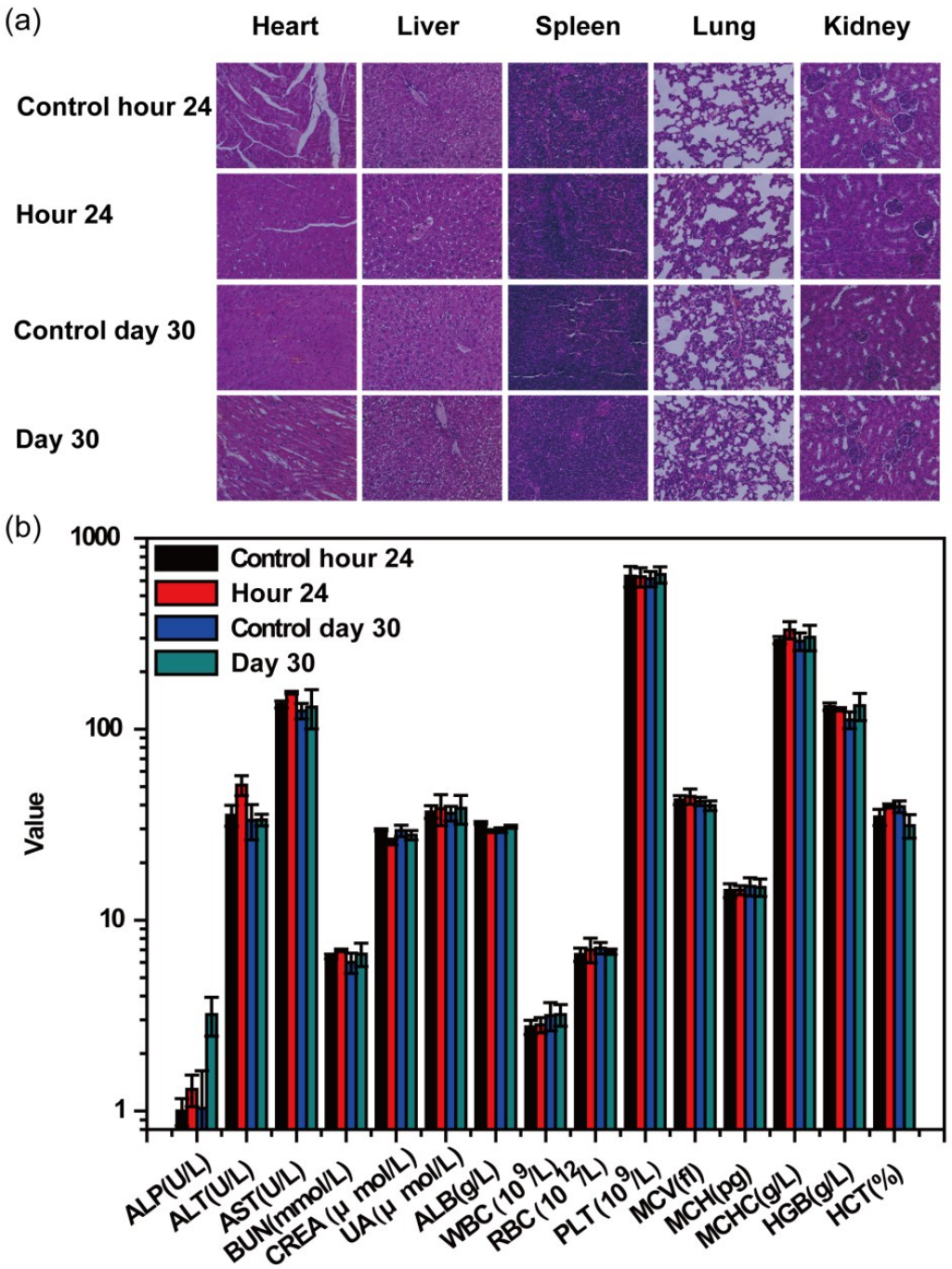

Fig. S26 (a) H&E stained organ slices collected from the mice after tail vein injection of saline (the control groups) and Ir-Dy HNPs for 24 h and 30 days, respectively. (b) Biochemical indices of blood obtained from the mice after tail vein injection of saline (the control groups) and Ir-Dy HNPs for 24 h and 30 days, respectively. Where ALP is alkaline phosphatase; ALT is Alanine aminotransferase; AST, is aspartate aminotransferase; BUN is blood urea nitrogen; CREA is creatinine; UA is uric acid; ALB is albumin; RBC is red blood cells; WBC is white blood cells; MCV is mean corpuscular volume; PLT is platelet; MCHC is mean corpuscaular haemoglobin concentration; MCH is mean corpuscular hemoglobin; HCT IS red blood cell specific volume; HGB is haemoglobin.

References

[1] F. Xue, Y. Lu, Z. Zhou, M. Shi, Y. Yan, H. Yang and S. Yang, *Organometallics*, 2015, **34**, 73-77.

[2] Q. Wang , H. Wang , W. Yang, D. Wang and Y. Ding, *Inorg. Chem. Commun.* 2013, **36**, 184-187